

DAMPING ENHANCEMENT OF A PROPOSED HELICOPTER BLADE-SAILING AEROSERVOELASTIC SYSTEM USING INDIVIDUAL BLADE ROOT CONTROL

Roberto Luiz da Cunha Barroso Ramos, rlcbramos@gmail.com

Donizeti de Andrade, donizeti@ita.br

Luiz Carlos Sandoval Góes, goes@ita.br

Technological Institute of Aeronautics, Aeroelastic Control Group, São José dos Campos, SP, Brazil

Abstract. *This paper analyzes the response of a proposed helicopter blade-sailing aeroservoelastic system with active damping enhancement based on individual blade root control. The designed flap-rate-feedback controller, in the rotating frame, yields active lift compensation through a blade pitch angle variation at the blade root, increasing the damping of the flapping motion without rotor design changes. The objective is the reduction of flapping deflections and the suppression of tunnel strikes for articulated rotors, considering steady-flow conditions during engagement shipboard operations. The aeroservoelastic modeling includes a nonlinear structural dynamics related to the droop and flap stops, blade-element aerodynamics with reverse-flow effects, a linear gust model for the ship airwake, gravity effects and an active lift compensator based on individual blade root control with actuator constraints. The aeroservoelastic analysis and design focus on the performance of the proposed individual-blade-root controller with respect to the reduction of blade flapping vibrations in high wind conditions. The closed-loop blade-sailing dynamics constitutes a pitch-controlled flapping oscillator with nonlinear stiffness and time-varying coefficients and it is simulated for an articulated rotor whose properties are based on the H-46 shipboard rotor. The simulation results show that the damping enhancement of the proposed aeroservoelastic system yields tunnel-strike suppression and it is associated with blade-sailing reduction of nearly 35% in upward deflections and nearly 20% in downward deflections at severe steady-flow wind-over-deck conditions, by using blade root-actuator limits of $\pm 6^\circ$.*

Keywords: *helicopter, blade sailing, individual blade root control, aeroservoelasticity, damping, shipboard operations.*

1. INTRODUCTION

Flexible rotating structures operating in high winds, such as helicopter rotors and wind turbines, are subjected to significant flow-induced loads which can yield large vibrations and damage. Shipboard helicopters, operating in the hostile maritime environment from frigate-like platforms, are especially susceptible to a dangerous phenomenon called *blade sailing*.

Blade sailing is an aeroelastic transient phenomenon characterized by the occurrence of large flapping vibrations, possibly associated with tunnel/tail-boom strikes (blade-fuselage impacts), due to fluid-structure interactions during engagement or disengagement operations of helicopter rotors under high wind conditions (Newman, 1995).

The blade-sailing control problem has a practical importance due the ubiquitous use of the shipboard helicopter in littoral defense missions (Wall *et al.*, 1995). Aeroservoelastic strategies, aimed at prescribing a low-vibration behavior for rotors operating in high winds, can yield active flow-induced load alleviation by using embedded blade controllers, sensors and actuators integrated according to a feedback control system. Previous research on active blade-sailing control includes swashplate-actuation for gimballed rotors (Keller, 2001), use of trailing-edge flaps (Jones and Newman, 2007) and active twist (Khouli *et al.*, 2008).

Considering that these active control concepts are not fully mature yet, the present work investigates the performance in steady flow of a new approach to helicopter blade-sailing reduction based on Theoretical Rotary-Wing Aeroservoelasticity (RWASE) and Individual Blade Root Control (IBRC). IBRC-based actuation, in the rotating frame, can yield reliable helicopter vibration reduction and allows the compensation of aerodynamic forces by superimposing a blade pitch angle variation at the blade root to the collective/cyclic commands (Haber *et al.*, 2002). The proposed design-oriented RWASE-IBRC approach is aimed at developing a blade-sailing model amenable to (Ramos, 2007) (Ramos *et al.*, 2008, 2009a, 2009b, 2009c):

- (1) Identify the flow-induced loads that govern the flapping vibrations (aeroservoelastic modeling).
- (2) Study active IBRC methods for shipboard rotors, in order to reduce the blade-sailing vibrations and enlarge the engagement/disengagement operating envelopes (aeroservoelastic analysis and design).

From the obtained aeroservoelastic model, a flap-rate-feedback individual-blade-root controller is proposed for the active damping enhancement of the flapping motion, including aerodynamic reverse-flow effects. The objective is the reduction of flapping deflections and the suppression of tunnel strikes for articulated rotors, considering steady-flow conditions during engagement shipboard operations. The closed-loop blade-sailing dynamics constitutes a pitch-controlled flapping oscillator with nonlinear stiffness and time-varying coefficients and it is simulated for an articulated rotor whose properties are based on the H-46 shipboard rotor. The aeroservoelastic analysis and design focus on the performance of the proposed flap-rate-feedback controller considering the IBRC blade pitch actuator limits.

2. AEROSERVOELASTIC MODELING

The aeroservoelastic modeling according to the proposed RWASE-IBRC approach includes a nonlinear structural dynamics related to the droop and flap stops, blade-element aerodynamics with reverse-flow effects, a linear gust model for the ship airwake, gravity effects and an active lift compensator based on individual blade root control with actuator constraints. Figures 1 and 2 illustrate the proposed blade-sailing aeroservoelastic scheme and control system, respectively.

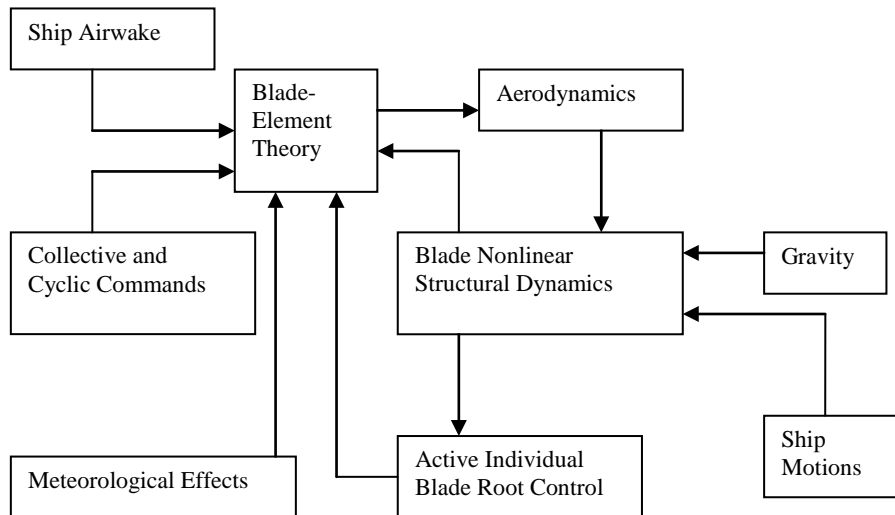


Figure 1. Block diagram of the proposed blade-sailing aeroservoelastic scheme

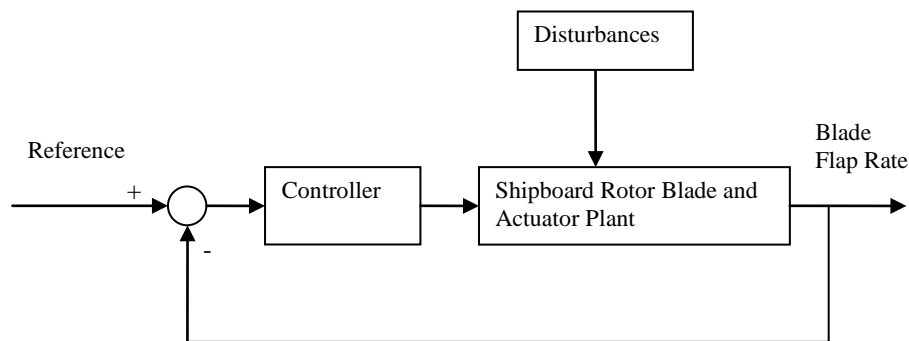


Figure 2. Block diagram of the proposed blade-sailing feedback control system

Figure 1 shows that the aerodynamic effects due to the ship airwake, collective/cyclic commands, meteorology, rotor blade motions and active individual blade root control input can be computed according to the blade-element theory, yielding flow velocities and an equivalent angle of attack, which determine the aerodynamic loads. These loads in conjunction with gravity and ship motion effects drive the blade nonlinear structural response and, thus, the blade pitch control input.

Figure 2 shows a feedback control system perspective, where the rotor blade loads due to aerodynamic effects, gravity and ship motions are viewed as disturbances to the plant constituted by the blade itself and its individual root actuator. The blade control input is computed according to a flap-rate-feedback strategy and generates a compensating aerodynamic moment for the flapping damping enhancement and vibration reduction. The choice of an individual blade control approach is due to the very different aerodynamic conditions that a blade experiences while rotating in high wind conditions.

2.1. Structural modeling

The blade-sailing modeling is based on the proposed rotary-wing aeroservoelastic scheme applied to articulated shipboard rotor blades, according to Figs. 1 and 2, taking into account some simplifying assumptions.

Considering that torsion effects are not significant for blade-sailing modeling (Geyer *et al.*, 1998) and that the Coriolis forces are small during the low rotor rotational speed regime, reducing the effects of the flap-lag coupling, only the flapping degree of freedom is taken into account. The model considers fully-articulated rotors with droop and flap stops. The rotor blade flapwise bending stiffness and mass are assumed uniformly distributed. The airfoil section is uniform along the blade and assumed NACA 0012. Inflow and ground effects are neglected, due to the low thrust conditions during the engagement and disengagement rotor operations. Gravity effects are included, due to the low rotational speed regime of the rotor blade behavior. Ship motion effects are not included. Unsteady flow conditions are not considered, therefore the wind-over-deck (WOD) velocity components of the ship airwake depend only on the flight deck position.

Therefore, in order to carry out the control analysis and design, the proposed blade-sailing aeroservoelastic model is simplified by considering the forces and moments actuating only in the flapping plane. Figure 3 shows the forces at a blade element for the simplified blade-sailing planar model, according to a frame rotating with the blade.

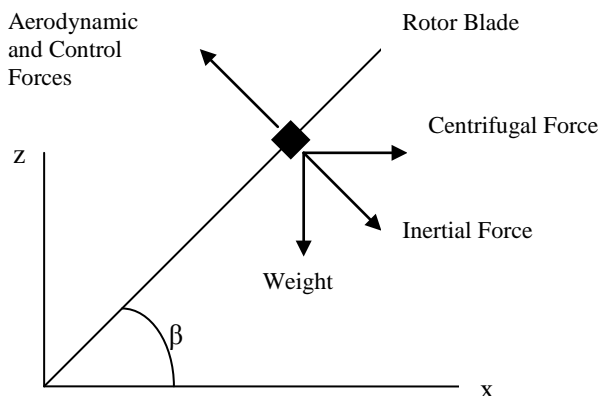


Figure 3. Forces at a flapping planar blade element for the proposed blade-sailing model (rotating frame)

The simplified diagram of forces at a planar blade element (Johnson, 1994) in Fig. 3 illustrates the main factors that govern the blade-sailing behavior. Ship motion effects are not included. The resulting moments about the flapping hinge in conjunction with the droop/flap stop effects, modeled as a nonlinear rotational spring (Ramos, 2007)(Ramos *et al.*, 2009a), determine the blade tip deflections related to the angle β .

From Fig. 3, the articulated-rotor blade-sailing dynamics is given by (Ramos, 2007)(Ramos *et al.*, 2009a):

$$\ddot{\beta} + \Omega^2 \beta + \sigma(\beta) = -\frac{3}{2R} g + \frac{M_{as} + M_{ac}}{I_B} \quad (1)$$

where

$$\begin{aligned} \sigma(\beta) &= \omega_{nr}^2 (\beta - \beta_{FS}), \text{ if } \beta > \beta_{FS} \\ \sigma(\beta) &= 0, \text{ if } \beta_{DS} \leq \beta \leq \beta_{FS} \\ \sigma(\beta) &= \omega_{nr}^2 (\beta - \beta_{DS}), \text{ if } \beta < \beta_{DS} \end{aligned} \quad (2)$$

In Eqs. (1) and (2), β is the blade flapping angle, Ω is the rotor rotational speed, $\sigma(\beta)$ is the nonlinear stiffness function related to the droop/flap-stop effects, R is the rotor radius, g is the acceleration of gravity, I_B is the blade moment of inertia about the center of rotation, M_{as} is the moment due to the aerodynamic forces related to the ship airwake, collective/cyclic commands and rotor blade motions, M_{ac} is the moment due to the aerodynamic active control forces, ω_{nr} is the blade non-rotating flapping natural frequency, β_{DS} is the blade droop stop angle, and β_{FS} is the blade flap stop angle.

2.2. Aerodynamic modeling: blade-element theory with reverse-flow effects

The three-dimensional ship airwake pattern can be modeled according to the mean ($\overline{V_x}, \overline{V_y}, \overline{V_z}$) and fluctuating (V'_x, V'_y, V'_z) flow velocity WOD components, as follows (Keller, 2001):

$$\begin{aligned} V_x &= \overline{V_x} + V'_x \\ V_y &= \overline{V_y} + V'_y \\ V_z &= \overline{V_z} + V'_z \end{aligned} \quad (3)$$

To simplify the aeroservoelastic analysis, only the lateral wind condition is considered, focusing the ship airwake modeling on the effects of the horizontal and vertical velocity components related to this worst-case blade-sailing condition (Newman, 1995). Therefore, the WOD mean longitudinal velocity component is neglected. For a typical frigate-like configuration with only one flight deck, as considered in this work, the WOD mean lateral velocity component can be considered uniform along the shipboard rotor.

The mean flow vertical velocity related to the interaction between the lateral undisturbed wind flow and a typical frigate-like structure can be approximated by a linear distribution along the flight deck and the helicopter rotor (Geyer *et al.*, 1998) (Newman, 1999). Therefore, for a rotor blade element at radial station r and azimuth Ψ , and uniform WOD mean lateral velocity component, the WOD mean vertical velocity, according to the linear distribution approximation (linear gust model), is given by:

$$\overline{V_z} = K_v \overline{V_y} \frac{r}{R} \sin \Psi \quad (4)$$

The gust factor K_v governs the flow-induced loads associated with the WOD vertical velocity component. Unsteady flow effects, despite their significance, are not considered for the aeroservoelastic analysis, therefore:

$$V'_x = V'_y = V'_z = 0 \quad (5)$$

The aerodynamic components affecting a shipboard rotor blade for the lateral wind condition can be calculated according to the blade-element theory, as follows (Keller, 2001):

$$\begin{aligned} U_T &= \Omega r - V_y \cos \Psi \\ U_P &= r\dot{\beta} + (V_y \sin \Psi)\beta - V_z \end{aligned} \quad (6)$$

In Eq. (6), U_P and U_T are, respectively, the normal and tangential flow velocity components at the blade element at radial station r , azimuth Ψ and flapping angle β . These flow velocity components are illustrated in Fig. 4, according to the blade-element theory (Dowell *et al.*, 1995). $V_z(r, \Psi)$ is the WOD vertical velocity at a blade element and $\Omega(t)$ is the time-varying rotational speed during shipboard engagement or disengagement operations.

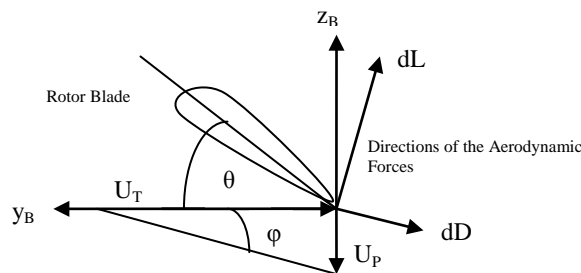


Figure 4. Aerodynamic forces and flow velocities at a blade element

The flapping aerodynamic moment can be obtained from the blade-element theory, as follows (Johnson, 1994):

$$M_{as} = \frac{1}{2} \rho a c \int_0^R (\theta U_T^2 - U_p U_T) r dr \quad (7)$$

where ρ is the air density, a is the slope of the lift coefficient curve, c is the blade chord, and θ is the blade pitch angle. Considering that:

$$I_B = \frac{mR^3}{3}; \quad \gamma \equiv \frac{3\rho a c R}{m}; \quad \mu_y \equiv \frac{V_y}{\Omega R} \quad (8)$$

where m is the blade mass per unit length, γ is the Lock number and μ_y is the advance ratio parameter, Eq. (8) yields for the blade aerodynamic moment, considering the lateral starboard side wind condition:

$$M_{as} = M_{ai} + M_{atw} + M_{a\dot{\beta}} + M_{a\beta} + M_{az} \quad (9)$$

where:

$$\begin{aligned} M_{ai} &= I_B \frac{\gamma \Omega^2}{8} \left[1 - \frac{8}{3} (\mu_y \cos \Psi) + 2 (\mu_y \cos \Psi)^2 \right] \theta_i \\ M_{atw} &= I_B \frac{\gamma \Omega^2}{2} \left[\frac{1}{5} - \frac{1}{2} (\mu_y \cos \Psi) + \frac{1}{3} (\mu_y \cos \Psi)^2 \right] \theta_{tw} \\ M_{a\dot{\beta}} &= I_B \frac{\gamma \Omega}{8} \left[-1 + \frac{4}{3} (\mu_y \cos \Psi) \right] \dot{\beta} \\ M_{a\beta} &= I_B \frac{\gamma \Omega^2}{8} \left[-\frac{4}{3} (\mu_y \sin \Psi) + (\mu_y^2) \sin 2\Psi \right] \beta \\ M_{az} &= I_B \frac{\gamma \Omega}{8R} \left\{ \left[1 - \frac{4}{3} (\mu_y \cos \Psi) \right] V_{zg} + \left[\frac{4}{3} - 2 (\mu_y \cos \Psi) \right] V_{zu} \right\} \end{aligned} \quad (10)$$

and

$$\begin{aligned} \theta_i &= \theta_{.75} + \theta_{1s} \sin \Psi + \theta_{1c} \cos \Psi - \frac{3}{4} \theta_{tw} \\ V_{zg} &= K_v V_y \sin \Psi \\ V_{zu} &= 0 \end{aligned} \quad (11)$$

The parameters $\theta_{.75}$, θ_{1s} , θ_{1c} and θ_{tw} are, respectively, the blade collective, longitudinal cyclic, lateral cyclic and the linear built-in twist angles. The terms M_{ai} , M_{atw} , $M_{a\dot{\beta}}$, $M_{a\beta}$, M_{az} are, respectively, the aerodynamic moments due to the blade pitch input, to the blade built-in twist, to the blade flapping rate, to the blade flapping angle, and to the WOD vertical velocity.

The rotor rotational speed Ω is not constant during engagement/disengagement operations, thus, the blade azimuth Ψ in Eq. (10) is not simply given by $\Psi = \Omega t$. The adopted rotational speed profile is based on the shipboard rotor engagement characteristics of the H-46 Sea Knight helicopter (Keller, 2001).

Obviously, the advance ratio parameter related to the lateral WOD component μ_y also varies with time. The aerodynamic moments associated with the flapping angle and rate in Eq. (10) introduce time-varying coefficients on the blade flapping motion/blade-sailing equation.

Considering the large reverse-flow region at the retreating side of the rotor disk, due to the high wind velocities in conjunction with the low rotational speeds during rotor engagement/disengagement, the aerodynamic moments given by Eq. (10) must be corrected for the retreating blade motion based on (Johnson, 1994). The corresponding aerodynamic moments are given by:

$$\begin{aligned}
 M_{ai} &= I_B \frac{\gamma \Omega^2}{8} \left[1 - \frac{8}{3} (\mu_y \cos \Psi) + 2 (\mu_y \cos \Psi)^2 - \frac{2}{3} (\mu_y \cos \Psi)^4 \right] \theta_i \\
 M_{atw} &= I_B \frac{\gamma \Omega^2}{2} \left[\frac{1}{5} - \frac{1}{2} (\mu_y \cos \Psi) + \frac{1}{3} (\mu_y \cos \Psi)^2 - \frac{1}{15} (\mu_y \cos \Psi)^5 \right] \theta_{tw} \\
 M_{a\dot{\beta}} &= I_B \frac{\gamma \Omega}{8} \left[-1 + \frac{4}{3} (\mu_y \cos \Psi) - \frac{2}{3} (\mu_y \cos \Psi)^4 \right] \dot{\beta} \\
 M_{a\beta} &= I_B \frac{\gamma \Omega^2}{8} \left[-\frac{4}{3} (\mu_y \sin \Psi) + (\mu_y^2) \sin 2\Psi - \frac{4}{3} (\mu_y \sin \Psi) (\mu_y \cos \Psi)^3 \right] \beta \\
 M_{az} &= I_B \frac{\gamma \Omega}{8R} \left\{ \left[1 - \frac{4}{3} (\mu_y \cos \Psi) + \frac{2}{3} (\mu_y \cos \Psi)^4 \right] V_{zg} + \left[\frac{4}{3} - 2 (\mu_y \cos \Psi) + \frac{4}{3} (\mu_y \cos \Psi)^3 \right] V_{zu} \right\}
 \end{aligned} \tag{12}$$

2.3. Active Individual Blade Root Control

Aerodynamic moments can be designed for the reduction of blade-sailing vibrations by using active control methods. As mentioned in the introduction, previous researches on blade-sailing active control were based on swashplate-actuation for gimbaled rotors (Keller, 2001), use of trailing-edge flaps (Jones and Newman, 2007) and active twist (Khouli et al., 2008).

The new active control approach proposed in this work for articulated shipboard rotors is based on Individual Blade Root Control (IBRC) actuation (Haber *et al.*, 2002). A variable length rod, constituted by a hydraulic actuator, is linked to the swashplate, in order to allow a blade pitch control input to superimpose the collective and cyclic commands. The hydraulic actuators replace the rigid pitch links of the helicopter control system, yielding IBRC motions, which can reduce rotor vibration.

Accelerometers and strain gauges can be used for sensing and approximate calculation of the blade flapping angle and angular velocity, based on the blade tip motion.

The IBRC method is associated with the rotating frame (Fig. 3), allowing the generation of compensating aerodynamic moments according to the individual behavior of each rotor blade. This characteristic is especially important for articulated rotors because droop/flap-stop impacts and tunnel/tail-boom strikes are the main concern about blade-sailing occurrences.

The aerodynamic moment associated with an angle-of-attack/lift compensation due to an IBRC pitch input θ_u , in the rotating frame, can be obtained from Eqs. (10) and (12), considering the term M_{ai} , as follows:

$$\begin{aligned}
 M_{ac} &= I_B \frac{\gamma \Omega^2}{8} \left[1 - \frac{8}{3} (\mu_y \cos \Psi) + 2 (\mu_y \cos \Psi)^2 \right] \theta_u, \text{ for the advancing blade motion} \\
 M_{ac} &= I_B \frac{\gamma \Omega^2}{8} \left[1 - \frac{8}{3} (\mu_y \cos \Psi) + 2 (\mu_y \cos \Psi)^2 - \frac{2}{3} (\mu_y \cos \Psi)^4 \right] \theta_u, \text{ for the retreating blade motion}
 \end{aligned} \tag{13}$$

Substituting the expressions given by Eqs. (9), (10), (12), and (13) into Eq. (1), yields:

$$\ddot{\beta} + c_{\dot{\beta}}(t)\dot{\beta} + c_{\beta}(t)\beta + \sigma(\beta) = u(t) + x_0(t) \tag{14}$$

where $c_{\dot{\beta}}(t)$, $c_{\beta}(t)$ are the damping and stiffness time-varying coefficients, respectively, $\sigma(\beta)$ is the nonlinear stiffness function related to the droop/flap-stop effects, $u(t)$ represents the active IBRC input and $x_0(t)$ represents the exogenous inputs due to the ship airwake, to the pilot commands, to the blade twist and to gravity. According to Eq. (14), the single-degree-of-freedom blade-sailing behavior is governed by a nonlinear ordinary differential equation with time-varying coefficients.

Considering $x = [\beta \quad \dot{\beta}]^T = [x_1 \quad x_2]^T$, the active aeroelastic control analysis and design can be simplified by using a state-space model obtained from Eq. (14), as follows:

$$\begin{aligned}
 \dot{x}_1 &= x_2 \\
 \dot{x}_2 &= -c_{\dot{\beta}}(t)x_2 - c_{\beta}(t)x_1 - \sigma(x_1) + u(t) + x_0(t)
 \end{aligned} \tag{15}$$

2.4. Model verification and analysis

The verification of the obtained blade-sailing model is carried out by comparison with results given in (Geyer *et al.*, 1998) from a model validated with experimental data, by using a fourth-fifth order Runge-Kutta numerical simulation. The helicopter rotor parameter values for the simulations are shown in Tab. 1:

Table 1. H-46 Sea Knight shipboard helicopter parameters

γ (Lock number)	7.96
Ω_0 (nominal rotor rotational speed)	27.65 rad/s
V_y (lateral WOD velocity)	- 20.4 m/s
V_x (longitudinal WOD velocity)	0 m/s
R (rotor radius)	7.77 m
ω_{nr} (blade non-rotating flapping frequency)	6 rad/s
β_{DS} (droop stop angle)	- 1°
B_{FS} (flap stop angle)	1°
θ_{75} (collective pitch angle)	3°
θ_{tw} (built-in twist angle)	- 8.5°
θ_{1s} (longitudinal cyclic angle)	2.5°
θ_{1c} (lateral cyclic angle)	0.0693°

A numerical simulation is carried out for the linear gust model of the ship airwake and Fig. 5 illustrates the results.

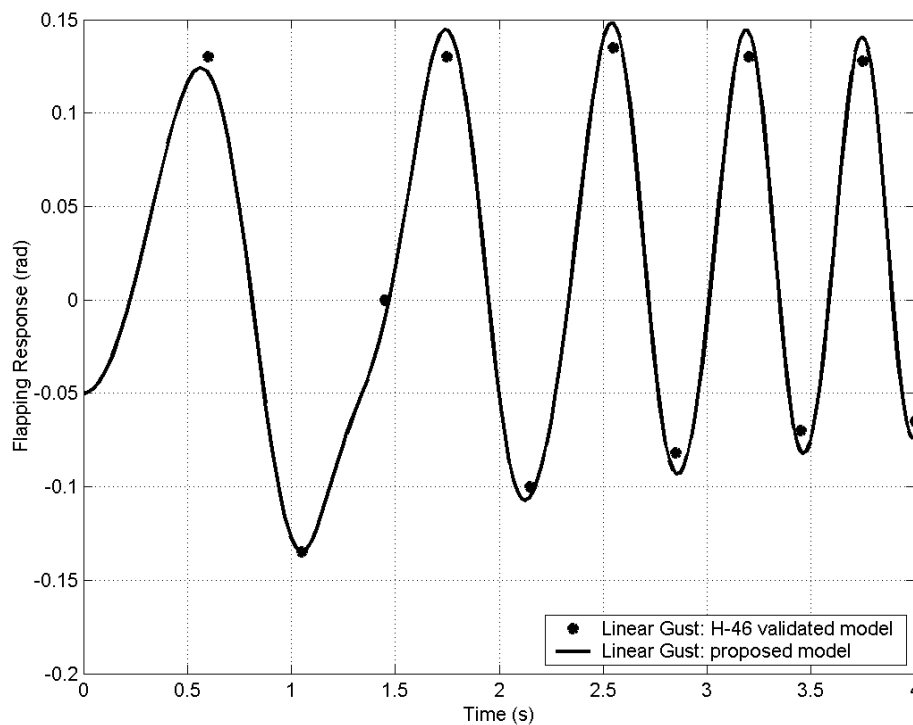


Figure 5. Flapping response for the linear gust model

The flapping response diagram in Fig. 5 shows a very good agreement of the proposed model with the results given in (Geyer *et al.*, 1998). The time range 0-4 seconds of the simulation corresponds to 6-10 seconds for the actual H-46 engagement behavior, when rotor rotational speeds are low, varying from 10% to 46% of the nominal rotation speed (NR).

3. AEROSERVOELASTIC ANALYSIS AND DESIGN

The active aeroelastic controller design is based on the obtained blade-sailing model, considering a nominal steady-flow condition associated with tunnel-strike occurrences for the H-46 shipboard helicopter (blade tip deflections greater than 18%R). The proposed IBRC-based actuation in the rotating frame can modify the angle of attack and, hence, the lift conditions at the blade sections, by superimposing a blade pitch input at the root to the collective/cyclic commands. *This active lift compensation can be associated with the damping enhancement of the flapping motion by using a flap-rate-feedback control law.* Therefore, the blade pitch control input θ_u is given by:

$$\theta_u = -K_d \dot{\beta} \quad (16)$$

where K_d is the active control parameter.

The proposed Flap-Rate-Feedback Individual-Blade-Root-Control (IBRC) strategy generates compensating aerodynamic moments that are related to the enhancement of the flapping damping according to the active control parameter K_d , replacing passive flapping dampers.

Therefore, the proposed IBRC strategy allows the tuning of the individual blade aerodynamic conditions associated with the blade tip oscillations. The IBRC-based active pitch control design, involving the control parameter estimation, can be accomplished by using physical and mathematical principles concerning the desired damping properties of the blade flapping closed-loop oscillator, that is, *the flap-rate-feedback control design problem consists on finding a suitable range for the parameter K_d , aiming at achieving closed-loop damping features compatible with safe blade-sailing vibrations at the nominal steady-flow tunnel-strike condition. An important requirement for actual operations is that the control inputs must not be excessive, in order to avoid actuator saturation problems.* For this study, the blade pitch control inputs from the actuators are limited to $\pm 6^\circ$ (Haber *et al.*, 2002).

One can observe that, for a positive control parameter, the compensating aerodynamic moment adds damping to the flapping dynamics. This additional damping shall reduce the downward and upward blade flapping deflections, considering the constraints on the actuators. Unfortunately, the use of analytical methods to design the proposed feedback controller subjected to input constraints is not feasible, due to the nonlinear time-varying non-autonomous characteristics of the obtained aeroservoelastic blade-sailing model. Therefore, numerical simulations based on physical and mathematical principles related to the desirable damping properties of the closed-loop flapping oscillator, guided by the theory of vibrations, are the best method to evaluate the effects on the blade-sailing response of a particular choice of the control parameter.

To obtain an initial estimate for the control parameter K_d , the aeroservoelastic blade-sailing model is simplified by approximating the time-varying coefficients by constant ones and by using a linear approximation for the nonlinear stiffness function $\sigma(\beta)$. Applying these approximations, the blade-sailing dynamics is given by:

$$\ddot{\beta} + \frac{\gamma\Omega}{8}(1 + K_d\Omega)\dot{\beta} + \Omega^2 \left(1 + \frac{\omega_{nr}^2}{\Omega^2}\right)\beta = x_0(t) \quad (17)$$

where $x_0(t)$ represents the forcing terms, due to the collective/cyclic commands, to the blade built-in twist, to flow effects, and to gravity. The rotor rotational speed Ω is assumed constant and equal to 20% of the nominal rotational speed (NR), determining the tunnel-strike condition for aeroelastic control design purposes. The approximate closed-loop dynamics can be represented by using a suitable form according to the theory of linear oscillations, as follows:

$$\ddot{\beta} + 2\zeta\omega_n\dot{\beta} + \omega_n^2\beta = x_0(t) \quad (18)$$

The control parameter is given by:

$$K_d = \frac{8}{\gamma\Omega^2}(2\zeta\omega_n) - \frac{1}{\Omega}, \quad \omega_n = \sqrt{\Omega^2 + \omega_{nr}^2} \quad (19)$$

Therefore, the control parameter K_d can be estimated from the desired damping parameter ζ of the approximate linear oscillator. The aeroservoelastic analysis of the blade-sailing nonlinear time-varying system is carried out considering tunnel-strike conditions at a lateral wind-over-deck velocity V_{WOD} equal to 25.5 m/s. The simulations consider damping parameter values from 0.4 to 1 for the approximate dynamics, corresponding to an IBRC parameter range of 1/NR to 10/NR. Figures 6 and 7 show the blade flapping response and the blade pitch control input, respectively, for K_d equal to 3/NR, which yields the largest flapping damping enhancement without actuator saturation.

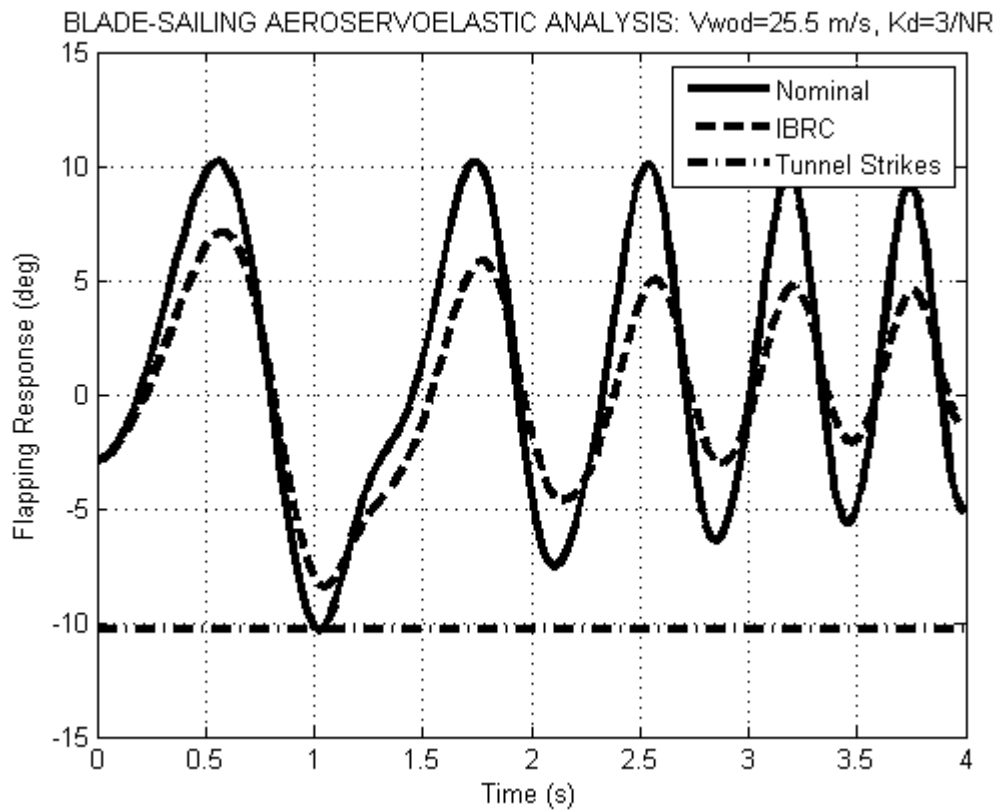


Figure 6. Flapping response – $K_d = 3/NR$

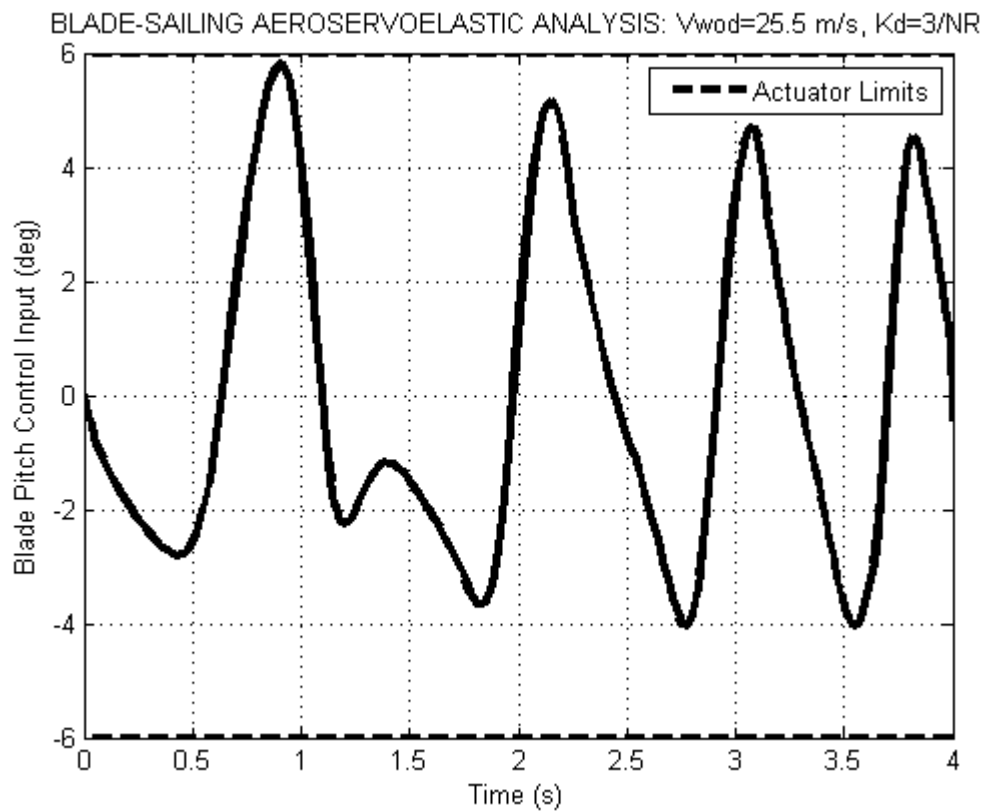


Figure 7. Blade pitch control input – $K_d = 3/NR$

4. CONCLUSIONS

1. The simulation results show that the proposed helicopter blade-sailing aeroservoelastic system using an IBRC-based strategy yields damping-enhancement effects associated with nearly 20% reduction in downward flapping deflections.
2. This downward flapping reduction is sufficient to avoid tunnel-strike occurrences at severe steady-flow wind-over-deck conditions.
3. The proposed IBRC-based aeroservoelastic system yields blade-sailing reduction of nearly 35% in upward deflections.
4. The proposed flap-rate-feedback IBRC-based strategy yields significant blade-sailing reduction without actuator saturation (limits of $\pm 6^\circ$).
5. Future work will involve the study of optimal/robust IBRC-based (active blade pitch control) strategies for blade-sailing mitigation in high winds.

5. ACKNOWLEDGEMENTS

The first author would like to thank CAPES for the partial funding of this research through the post-doctorate PRODOC program.

6. REFERENCES

- Dowell, E.H. *et al.* (ed.), 1995, "A Modern Course in Aeroelasticity - Chapter 7", Kluwer Academic, pp. 370-437.
- Geyer, J.R., Smith, E.C. and Keller, J.A., 1998, "Aeroelastic Analysis of Transient Blade Dynamics During Shipboard Engage/Disengage Operations", *Journal of Aircraft*, Vol. 35, No. 3, pp. 445-453.
- Haber, A., Jacklin, S.A. and DeSimone, G., 2002, "Development, Manufacturing, and Component Testing of An Individual Blade Control System For a UH-60 Helicopter Rotor", American Helicopter Society Aerodynamics, Acoustics, and Test and Evaluation Technical Specialists Meeting, San Francisco, CA, Proceedings.
- Johnson, W., 1994, "Helicopter Theory", Dover, pp. 1-767.
- Jones, M.P. and Newman, S.J., 2007, "A Method of Reducing Blade Sailing through the Use of Trailing Edge Flaps", 63th American Helicopter Society Annual Forum, Proceedings.
- Keller, J.A., 2001, "Analysis and control of the transient aeroelastic response of rotors during shipboard engagement and disengagement operations", Thesis (PhD), The Pennsylvania State University.
- Khouli, F., Wall, A.S., Langlois, R.G. and Afagh F.F., 2008, "Investigation of the Feasibility of a Proposed Hybrid Passive and Active Control Strategy for the Transient Aeroelastic Response of Helicopter Rotor Blades During Shipboard Engage and Disengage Operations", 64th American Helicopter Society Annual Forum, Proceedings.
- Newman, S.J., 1995, "The Verification of a Theoretical Helicopter Rotor Blade Sailing Method by Means of Windtunnel Testing", *The Aeronautical Journal of the Royal Aeronautical Society*, Vol. 99, No. 982, pp. 41-51.
- Newman, S.J., 1999, "A Theoretical Model for Predicting the Blade Sailing Behaviour of a Semi-Rigid Rotor Helicopter", *Vertica*, Vol. 14, No. 4, pp. 531-544.
- Ramos, R.L.C.B., 2007, "Aeroservoelastic Analysis of the Blade-Sailing Phenomenon in the Helicopter-Ship Dynamic Interface", Thesis (D.Sc.), Technological Institute of Aeronautics, Brazil.
- Ramos, R.L.C.B., de Andrade, D. and Góes, L.C.S., 2008, "Individual Blade Root Control of Helicopter Blade Sailing for Hingeless Shipboard Rotors", X Simpósio de Aplicações Operacionais em Áreas de Defesa (SIGE), Brazil.
- Ramos, R.L.C.B., de Andrade, D. and Góes, L.C.S., 2009, "Individual Blade Root Control of Helicopter Blade Sailing for Articulated Shipboard Rotors", American Helicopter Society 65th Annual Forum, Proceedings.
- Ramos, R.L.C.B., de Andrade, D. and Góes, L.C.S., 2009, "Aeroservoelastic Analysis of a Proposed Helicopter Blade-Sailing Feedback Control System in Unsteady Flow", 8th Brazilian Conference on Dynamics, Control and Applications.
- Ramos, R.L.C.B., de Andrade, D. and Góes, L.C.S., 2009, "Controle Aeroservoelástico Individual por Pá do Fenômeno de Blade Sailing para Helicópteros Embarcados *Hingeless*", Pesquisa Naval (SDM).
- Wall, A.S., Zan, S.J., Langlois, R.G. and Afagh F.F., 2005, "A Numerical Model for Studying Helicopter Blade Sailing in an Unsteady Airwake", Flow-Induced Unsteady Loads and the Impact on Military Applications – NATO Symposium, Proceedings.

7. RESPONSIBILITY NOTICE

The authors are the only responsible for the printed material included in this paper.